Sensitividade de física além do modelo padrão de oscilação de neutrinos

Physics Beyond the Standard Model with DUNE

Workshop Renafae
12 – 14 de julho de 2021

Célio Moura - UFABC, Brazil
Para a colaboração DUNE-BR

Based on CPT19 presentation for the DUNE Collaboration

Talk Overview

- ❑ DUNE
- ❑ Standard Oscillation Picture
- ❑ Physics Beyond the Standard Model at DUNE
    - ❑ NSI
- ❑ Simulation tools

CCNH CENTRO DE CIÊNCIAS NATURAIS E HUMANAS Universidade Federal do ABC

Universidade Federal do ABC

DUNE DEEP UNDERGROUND NEUTRINO EXPERIMENT

DUNE

DEEP UNDERGROUND NEUTRINO EXPERIMENT

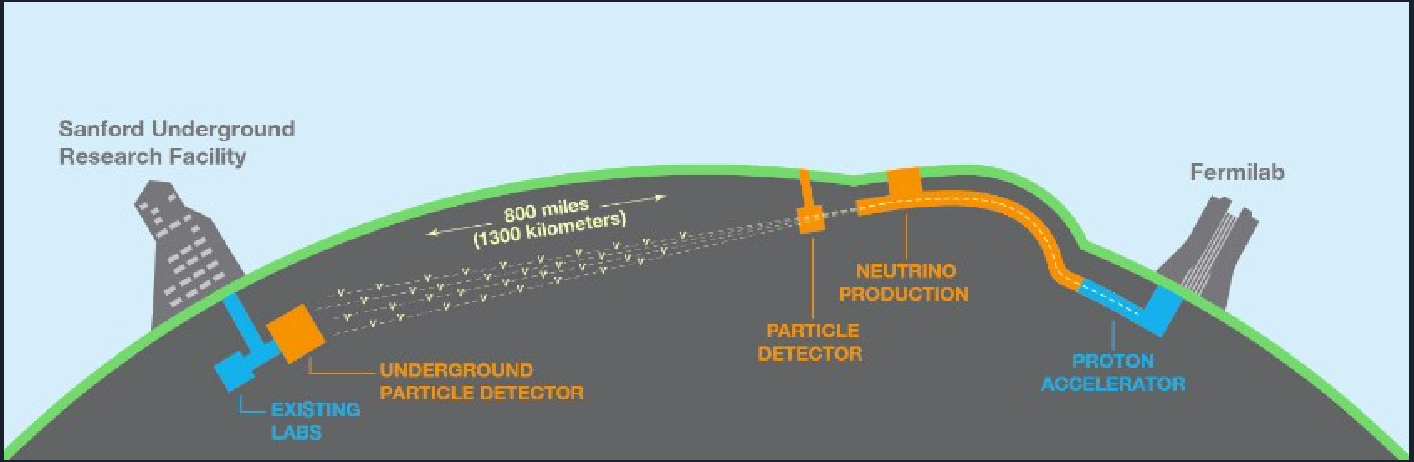

- Primary goals
  - CP phase
  - Mass ordering
  - Atmospheric mixing angle octant
- SN Burst
- Proton decay

DEEP UNDERGROUND
NEUTRINO EXPERIMENT

Fermilab accelerator complex

- 60-120 GeV proton beam at 1.2 MW, upgradeable to 2.4 MW
- Optimized for CP violation sensitivity
- Neutrino and antineutrino modes (~ GeV range).

DUNE DEEP UNDERGROUND NEUTRINO EXPERIMENT

DUNE Near Detector

Located approximately 575 m from neutrino source. Constrain systematic uncertainties for long-baseline oscillation analysis

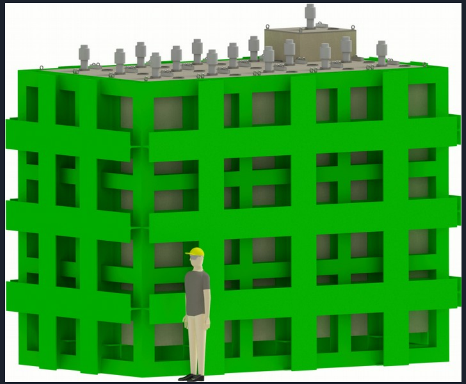

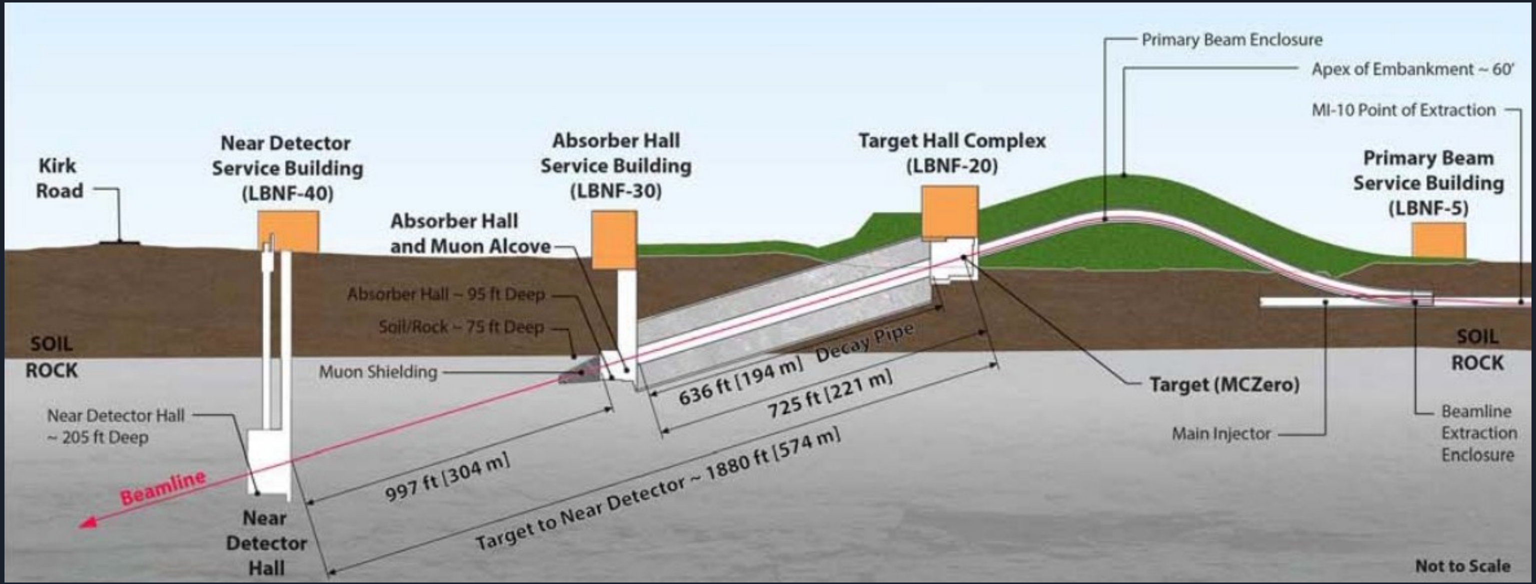

DUNE Far Detector

- ❑ Approximately 40 kt fiducial mass liquid-argon Far Detector.
- ❑ Located at SURF's 1478 m level with 1300 km baseline.

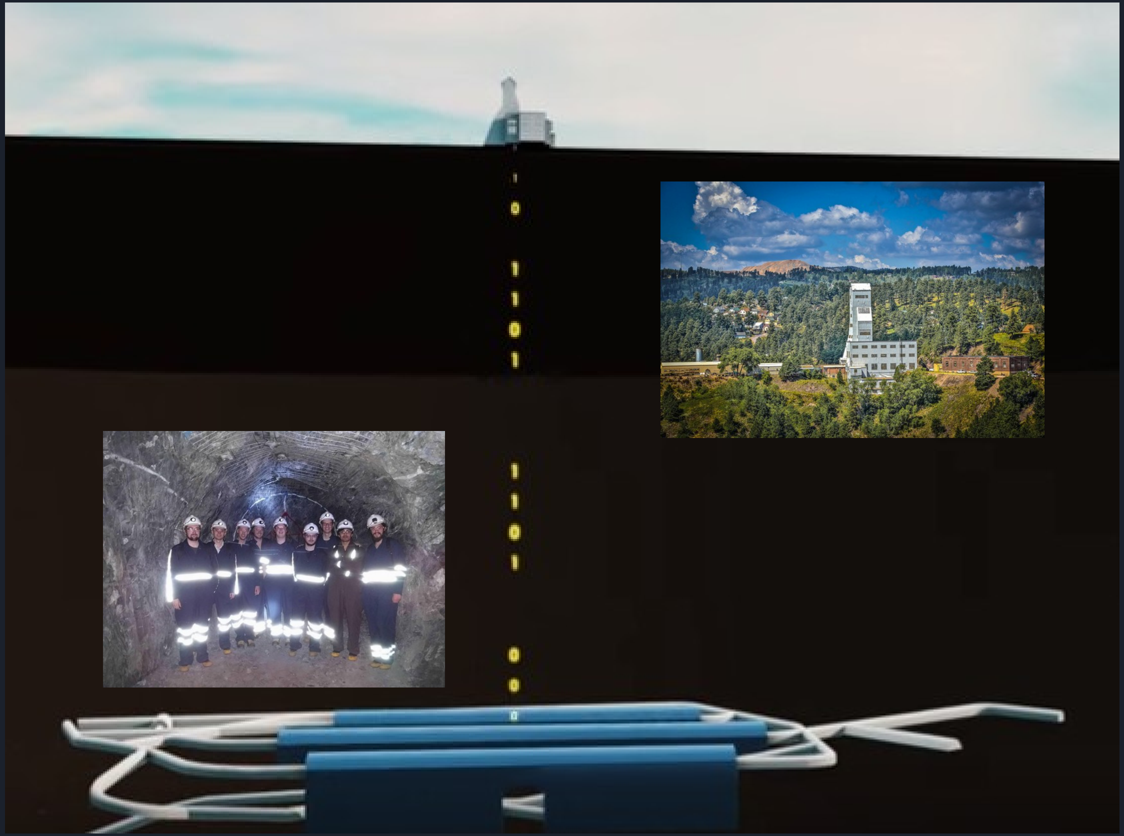

DUNE Far Detector
Also works for Supernova and Proton Decay

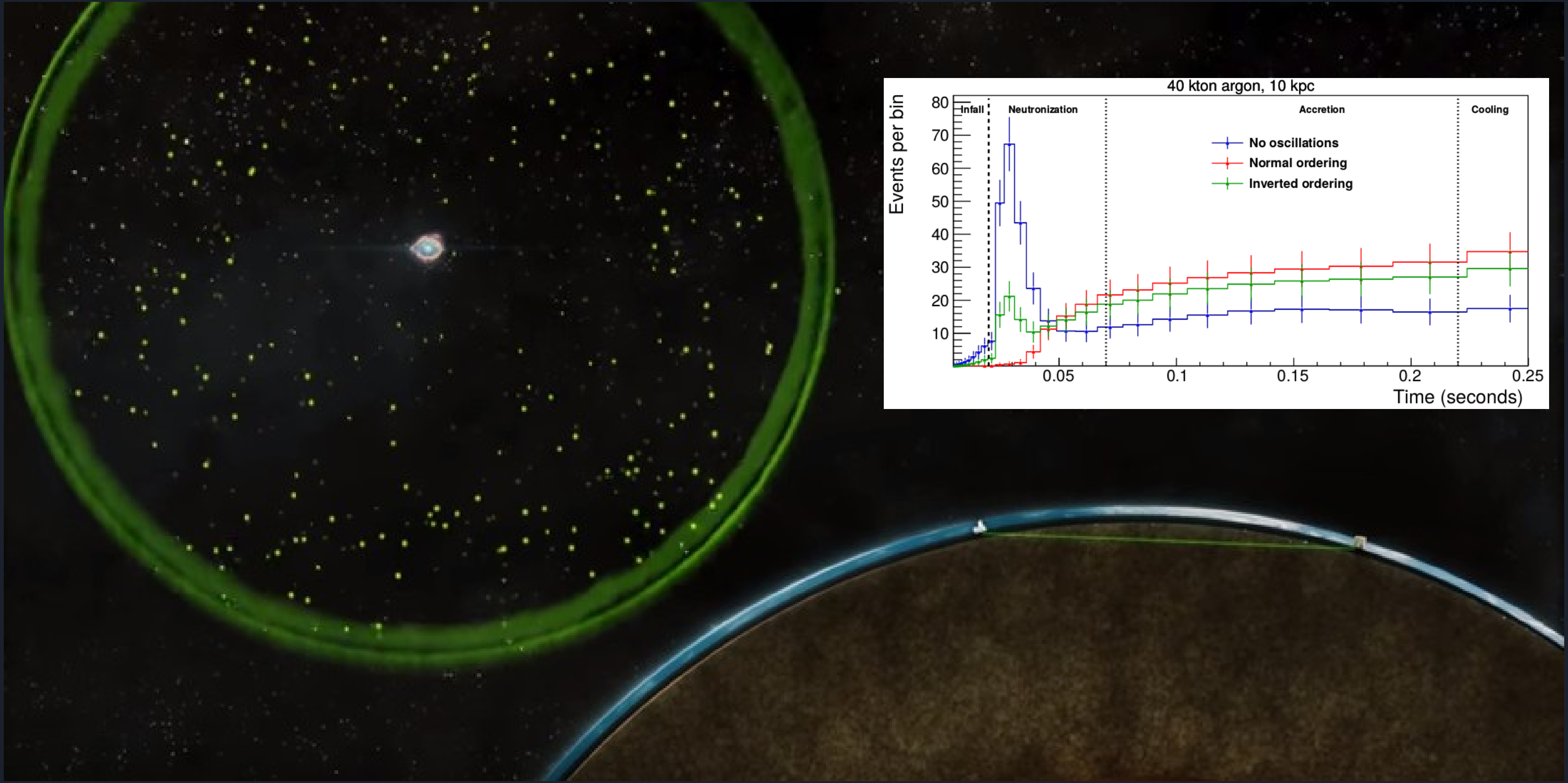

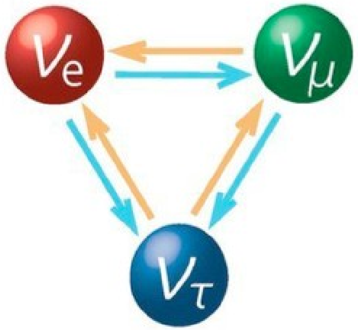

Neutrino oscillations

$$\begin{pmatrix} \nu_e \\ \nu_\mu \\ \nu_\tau \end{pmatrix} = \begin{pmatrix} c_{13}c_{12} & c_{13}s_{12} & s_{13}e^{-i\delta} \\ -c_{23}s_{12} - s_{13}s_{23}c_{12}e^{i\delta} & c_{23}c_{12} - s_{13}s_{23}s_{12}e^{i\delta} & c_{13}s_{23} \\ s_{23}s_{12} - s_{13}c_{23}c_{12}e^{i\delta} & -s_{23}c_{12} - s_{13}c_{23}s_{12}e^{i\delta} & c_{13}c_{23} \end{pmatrix} \begin{pmatrix} \nu_1 \\ \nu_2 \\ \nu_3 \end{pmatrix}$$

Neutrino vacuum oscillation parameters

$$P(\nu_\alpha \to \nu_\beta) = |\langle \nu_\beta | \nu_\alpha(t) \rangle|^2 \,.$$

$$i\frac{\partial}{\partial t}|\nu_k(t)\rangle = H_0|\nu_k(t)\rangle = E_k|\nu_k(t)\rangle \,,$$

$$\begin{aligned} P(\nu_\alpha \to \nu_\beta) \;&=\; \delta_{\alpha\beta} - 4\sum_{j>k}^{n} \mathrm{Re}\left(U_{\beta k}U^*_{\alpha k}U^*_{\beta j}U_{\alpha j}\right)\sin^2\left(\frac{\Delta m^2_{kj}}{4E}L\right) + \\ &\quad +2\sum_{j>k}^{n} \mathrm{Im}\left(U_{\beta k}U^*_{\alpha k}U^*_{\beta j}U_{\alpha j}\right)\sin\left(\frac{\Delta m^2_{kj}}{2E}L\right) \,. \end{aligned}$$

$$U_{\mathrm{PMNS}} = \begin{pmatrix} U_{e1} & U_{e2} & U_{e3} \\ U_{\mu 1} & U_{\mu 2} & U_{\mu 3} \\ U_{\tau 1} & U_{\tau 2} & U_{\tau 3} \end{pmatrix} = \begin{pmatrix} 1 & 0 & 0 \\ 0 & c_{23} & s_{23} \\ 0 & -s_{23} & c_{23} \end{pmatrix} \begin{pmatrix} c_{13} & 0 & s_{13}e^{-i\delta} \\ 0 & 1 & 0 \\ -s_{13}e^{i\delta} & 0 & c_{13} \end{pmatrix} \begin{pmatrix} c_{12} & s_{12} & 0 \\ -s_{12} & c_{12} & 0 \\ 0 & 0 & 1 \end{pmatrix}$$

Neutrino oscillation in matter

$$P(\nu_\alpha \to \nu_{\beta\neq\alpha}) = \sin^2(2\theta_M)\sin^2\left(\frac{\Delta m_M^2}{4E}L\right)$$

$$\Delta m_M^2 = \sqrt{(\Delta m^2\cos 2\theta - A(x))^2 + (\Delta m^2 \sin 2\theta)^2}$$

$$\sin 2\theta_M = \frac{\sin 2\theta \Delta m^2}{\sqrt{(\Delta m^2\cos 2\theta - A(x))^2 + (\Delta m^2 \sin 2\theta)^2}}\ .$$

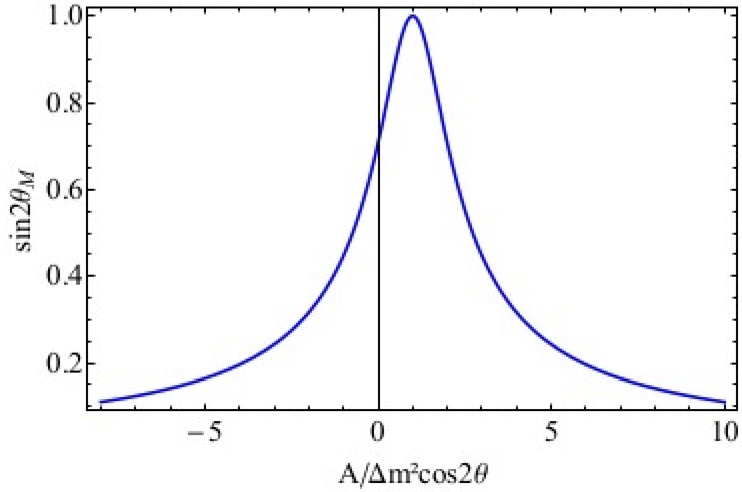

Three flavor oscillation probability

$$a = G_F N_e / \sqrt{2}$$

$$\Delta_{ij} = \Delta m_{ij}^2 L / 4E_\nu$$

$$P(\nu_\mu \to \nu_e) \simeq \sin^2\theta_{23}\sin^2 2\theta_{13}\frac{\sin^2(\Delta_{31}-aL)}{(\Delta_{31}-aL)^2}\Delta_{31}^2$$

$$+\sin 2\theta_{23}\sin 2\theta_{13}\sin 2\theta_{12}\frac{\sin(\Delta_{31}-aL)}{(\Delta_{31}-aL)}\Delta_{31}\frac{\sin(aL)}{(aL)}\Delta_{21}\cos(\Delta_{31}+\delta_{CP})$$

$$\cos^2\theta_{23}\sin^2 2\theta_{12}\frac{\sin^2(aL)}{(aL)^2}\Delta_{21}^2,$$

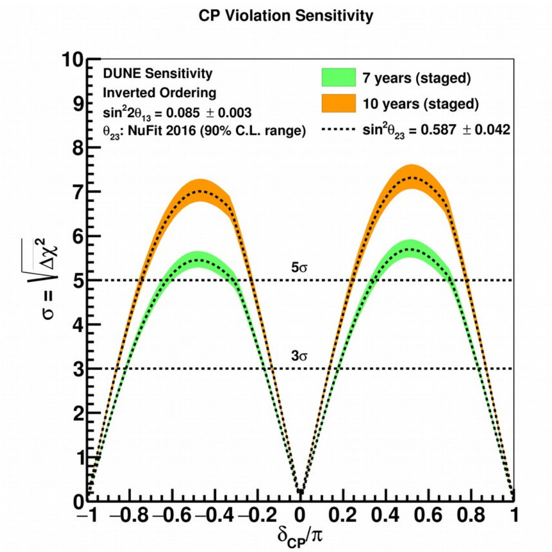

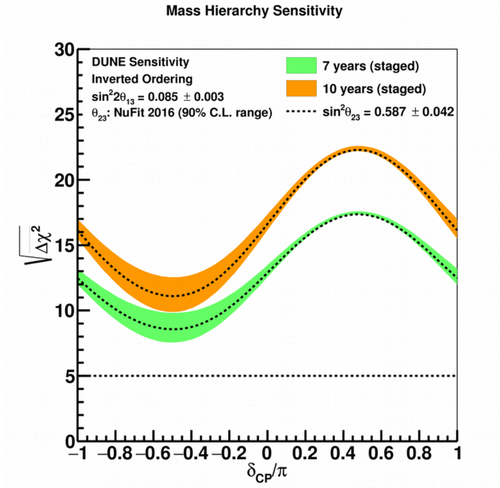

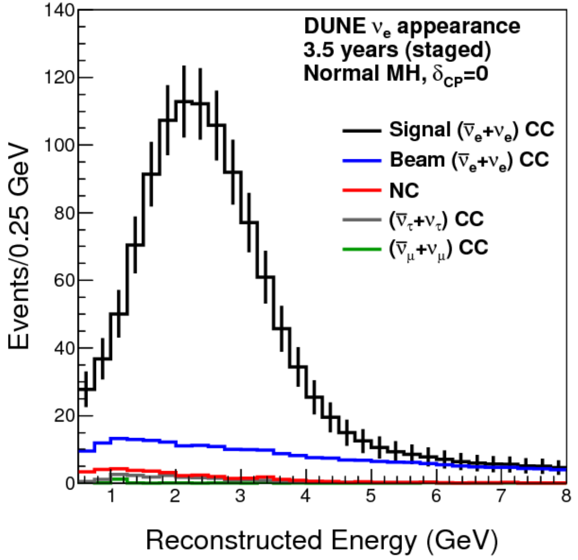

Oscillation probability for different channels

Different matter density profiles

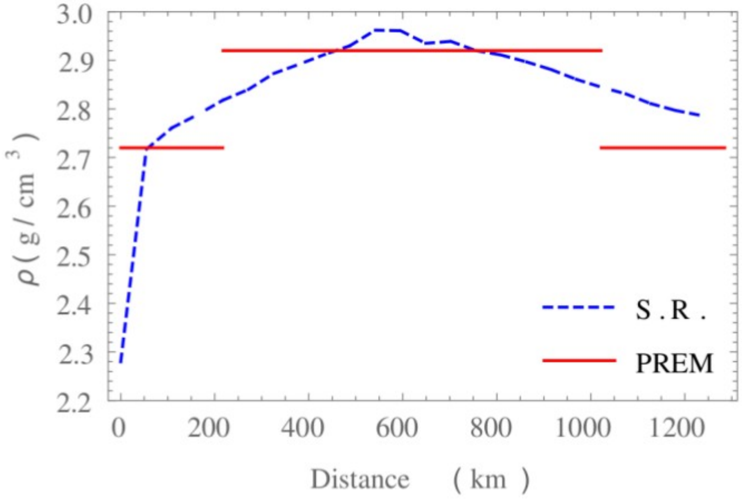

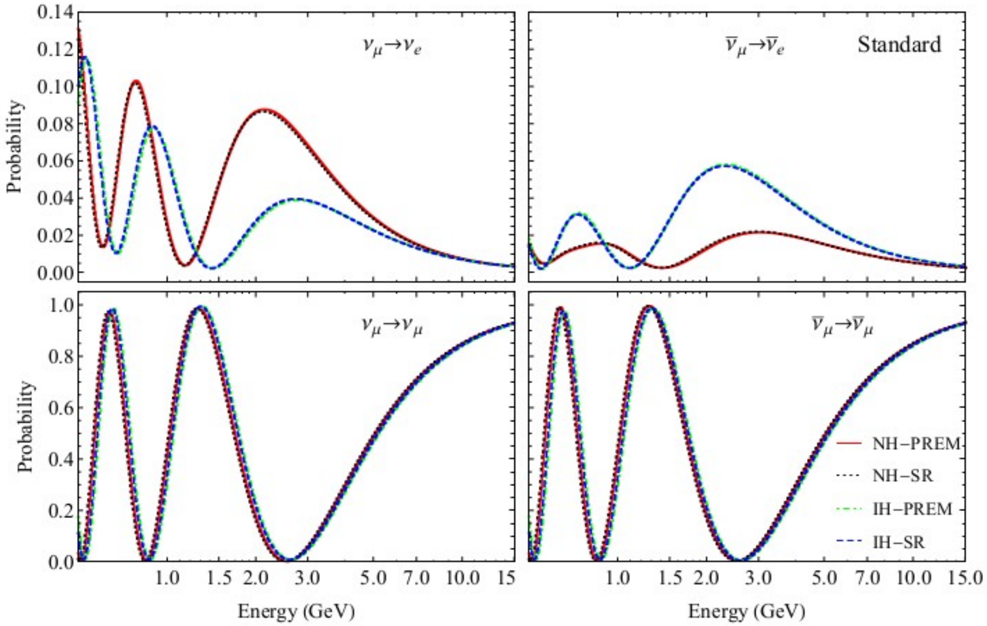

Normal and inverted mass hierarchies

BSM Physics

Focus on NSI

Different kinds of neutrino BSM interactions

NSI can affect neutrinos in production, detection and propagation processes

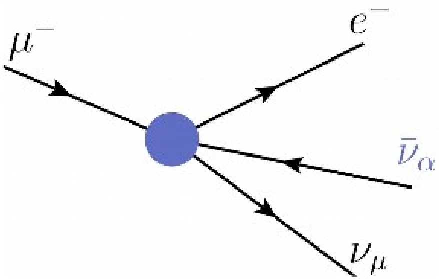

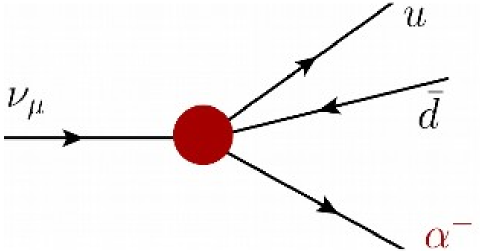

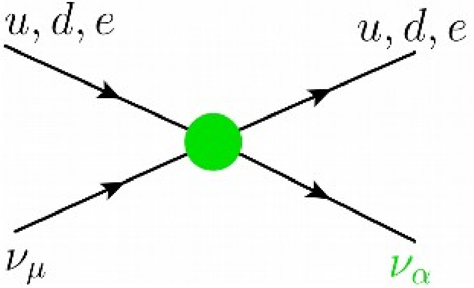

$\varepsilon^{e\mu}_{\mu\alpha} \left(\bar{e}\gamma^\rho \mu\right) \left(\bar{\nu}_\mu \gamma_{\rho,L} \nu_\alpha\right)$

$\varepsilon^{ud}_{\mu\alpha} V_{ud} \left(\bar{d}\gamma^\rho u\right) \left(\bar{\nu}_\mu \gamma_{\rho,L} \alpha\right)$

$\varepsilon^{f}_{\mu\alpha} \left(\bar{f}\gamma^\rho f\right) \left(\bar{\nu}_\mu \gamma_{\rho,L} \nu_\alpha\right)$

Near detectors

Far detectors

From P. Coloma presentation

New probabilities with NSI in the propagation

$$\mathcal{H} = \frac{1}{2E}\left\{U\begin{pmatrix} 0 & & \\ & \delta m_{21}^2 & \\ & & \delta m_{31}^2 \end{pmatrix}U^\dagger + 2EV_{CC}\begin{pmatrix} 1+\varepsilon_{ee} & \varepsilon_{e\mu} & \varepsilon_{e\tau} \\ \varepsilon_{e\mu}{}^\star & \varepsilon_{\mu\mu} & \varepsilon_{\mu\tau} \\ \varepsilon_{e\tau}{}^\star & \varepsilon_{\mu\tau}{}^\star & \varepsilon_{\tau\tau} \end{pmatrix}\right\}$$

The probability for $\nu_\mu \to \nu_\mu$ channel is given by

$$\begin{aligned} P_{\mu\mu}^{NSI} \simeq\ & 1 - s_{2\times23}^2\left[\sin^2\frac{\Delta_{31}L}{2}\right] \\ & - |\varepsilon_{\mu\tau}|\cos\phi_{\mu\tau}s_{2\times23}\left[s_{2\times23}^2(r_A\Delta_{31}L)\sin\Delta_{31}L + 4c_{2\times23}^2 r_A\sin^2\frac{\Delta_{31}L}{2}\right] \\ & + (|\varepsilon_{\mu\mu}| - |\varepsilon_{\tau\tau}|)s_{2\times23}^2 c_{2\times23}\left[\frac{r_A\Delta_{31}L}{2}\sin\Delta_{31}L - 2r_A\,\mathrm{si}\quad\frac{{}_{31}L}{2}\right], \end{aligned} \qquad (13)$$

where $s_{2\times23} \equiv \sin 2\theta_{23}$ and $c_{2\times23} \equiv \cos 2\theta_{23}$. Note that the NSI parameters involving the electron sector do not enter this channel and the survival probability depends only on the three parameters $\varepsilon_{\mu\mu}$, $\varepsilon_{\mu\tau}$, and $\varepsilon_{\tau\tau}$.

Appearance channel considering NSI

$$
\begin{aligned}
P_{e\mu}^{NSI} \;\simeq\;\; & 4s_{13}^2 s_{23}^2 \left[\frac{\sin^2(1-r_A)\Delta_{31}L/2}{(1-r_A)^2}\right] \\
& + 8s_{13}s_{23}c_{23}(|\varepsilon_{e\mu}|c_{23}c_\chi - |\varepsilon_{e\tau}|s_{23}c_\omega)\, r_A \left[\frac{\sin r_A\Delta_{31}L/2}{r_A}\;\frac{\sin(1-r_A)\Delta_{31}L/2}{(1-r_A)}\;\cos\frac{\Delta_{31}L}{2}\right] \\
& + 8s_{13}s_{23}c_{23}(|\varepsilon_{e\mu}|c_{23}s_\chi - |\varepsilon_{e\tau}|s_{23}s_\omega) r_A \left[\frac{\sin r_A\Delta_{31}L/2}{r_A}\;\frac{\sin(1-r_A)\Delta_{31}L/2}{(1-r_A)}\;\sin\frac{\Delta_{31}L}{2}\right] \\
& + 8s_{13}s_{23}^2(|\varepsilon_{e\mu}|s_{23}c_\chi + |\varepsilon_{e\tau}|c_{23}c_\omega) r_A \left[\frac{\sin^2(1-r_A)\Delta_{31}L/2}{(1-r_A)^2}\right]\;, \qquad (12)
\end{aligned}
$$

where $s_{ij} = \sin\theta_{ij}, c_{ij} = \cos\theta_{ij}$, $\Delta_{31} = \frac{\delta m^2{}_{31}}{2E}$, and $r_A = \frac{2EV_{CC}}{\delta m^2{}_{31}}$. Also, $c_\xi\ (s_\xi) = \cos\xi\ (\sin\xi)$

Oscillation Probability (E) for L ~ 1300 km

Only diagonal epsilons

Only e-tau epsilons

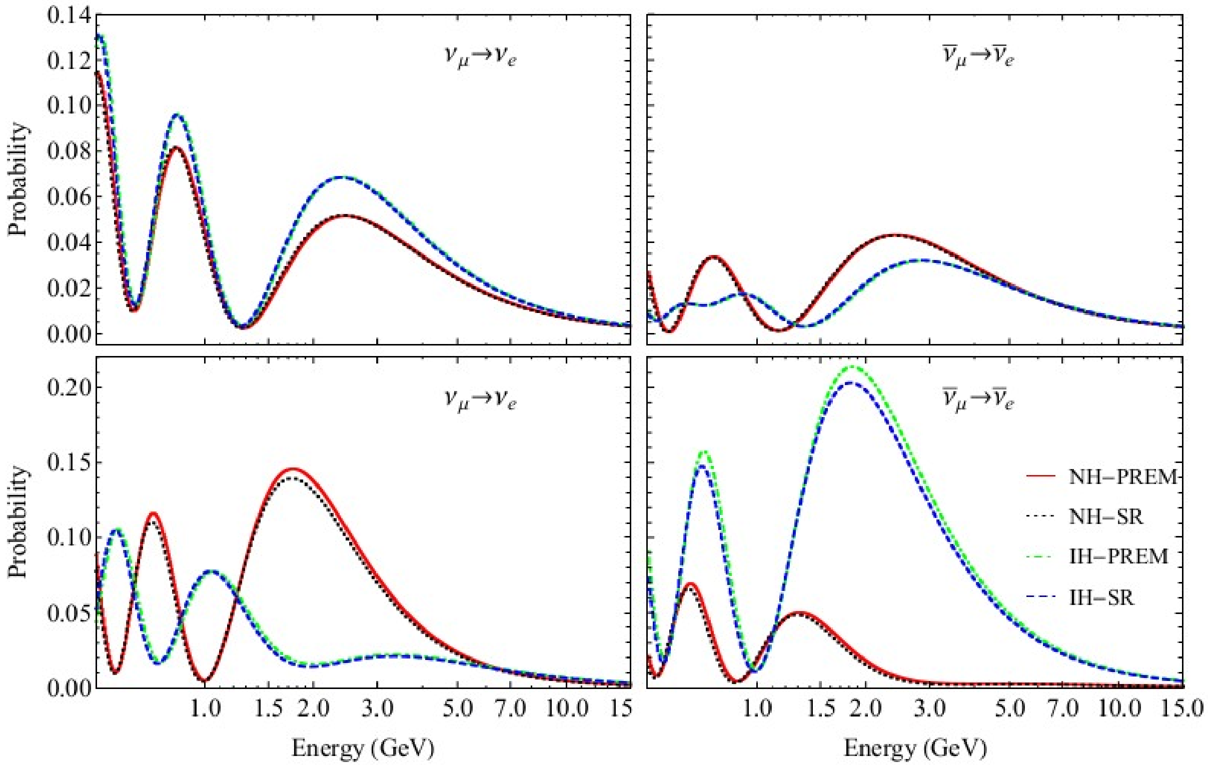

Event numbers for different NSI

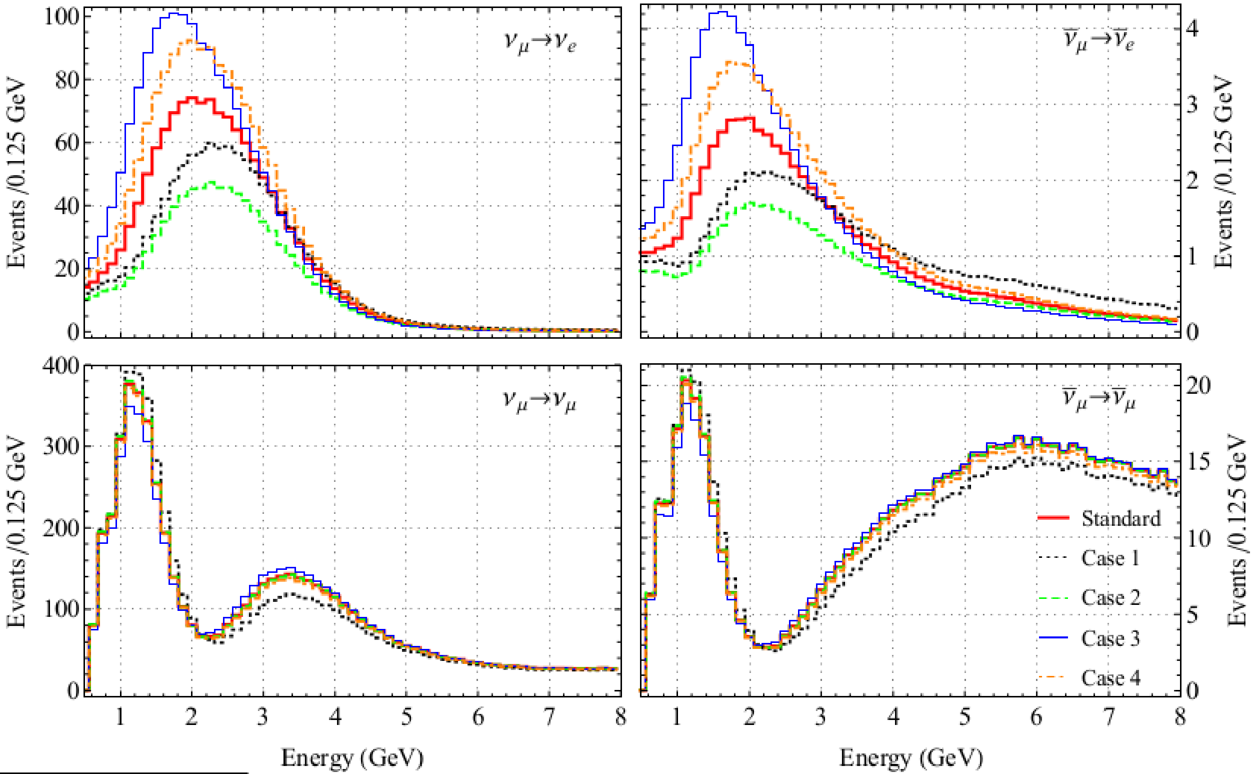

	ε_{ee}	$\varepsilon_{\tau\tau}$	$\lvert\varepsilon_{e\mu}\rvert$	$\lvert\varepsilon_{e\tau}\rvert$	$\lvert\varepsilon_{\mu\tau}\rvert$	$\phi_{e\mu}$	$\phi_{e\tau}$	$\phi_{\mu\tau}$
Case 1	0	0	0.15	0.3	0.05	$\pi/3$	$-\pi/4$	0
Case 2	-1.0	0.3	0	0	0	0	0	0
Case 3	0.5	-0.3	0	0.5	0	0	$\pi/3$	0
Case 4	0.5	0	0	0	0.2	0	0	$-\pi/2$

General concept of (GLoBES) simulation

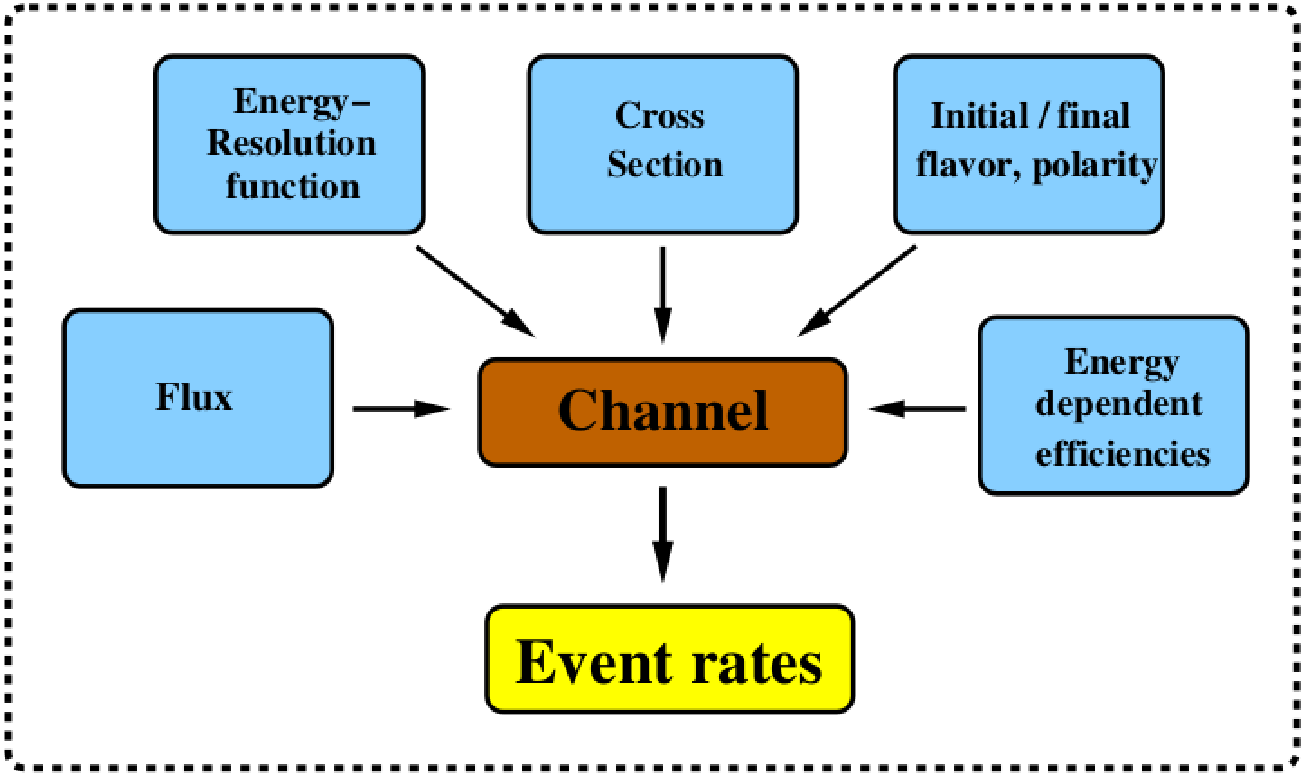

P. Huber at al.
https://www.mpi-hd.mpg.de/personalhomes/globes/

Different modules in GLoBES

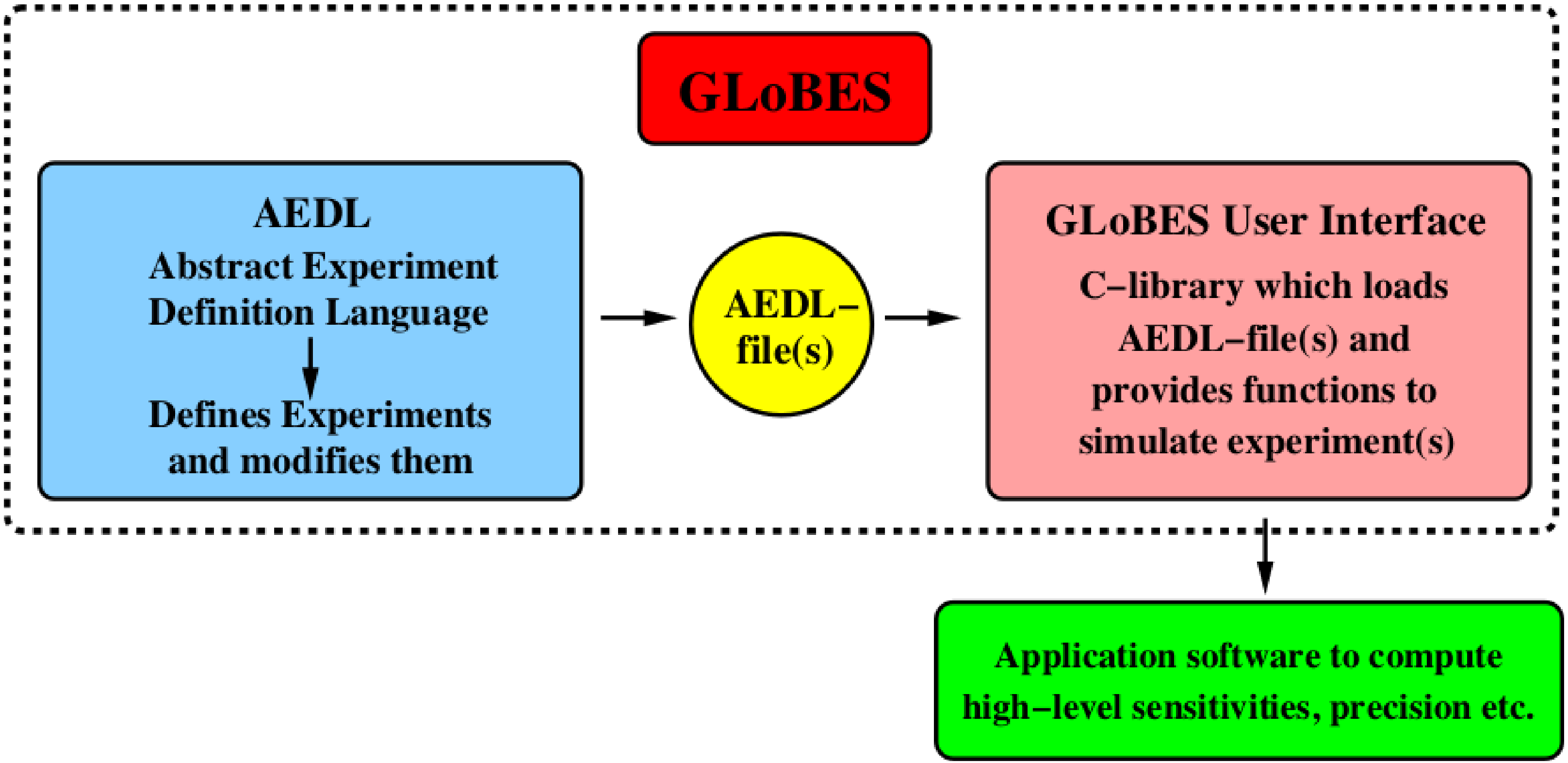

P. Huber at al. https://www.mpi-hd.mpg.de/personalhomes/globes/

NSI limits from DUNE and effects on sensitivity

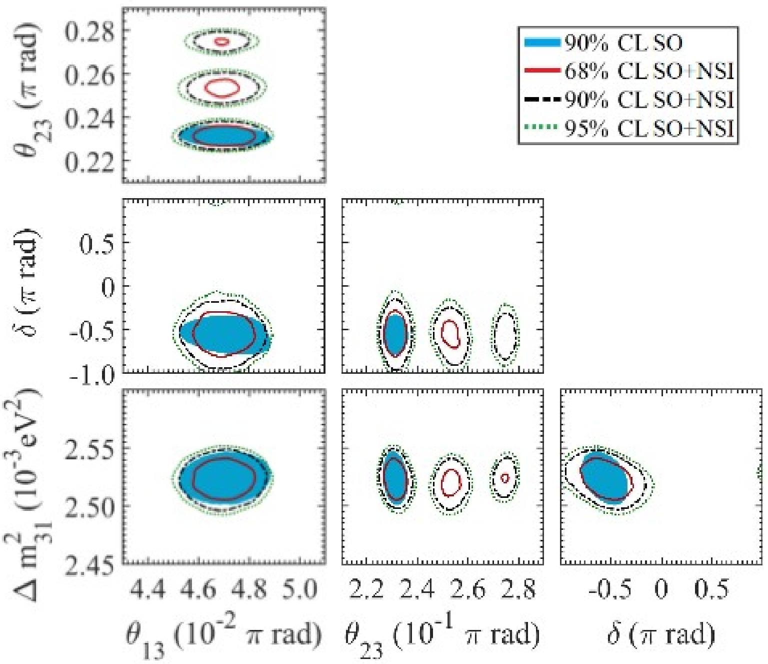

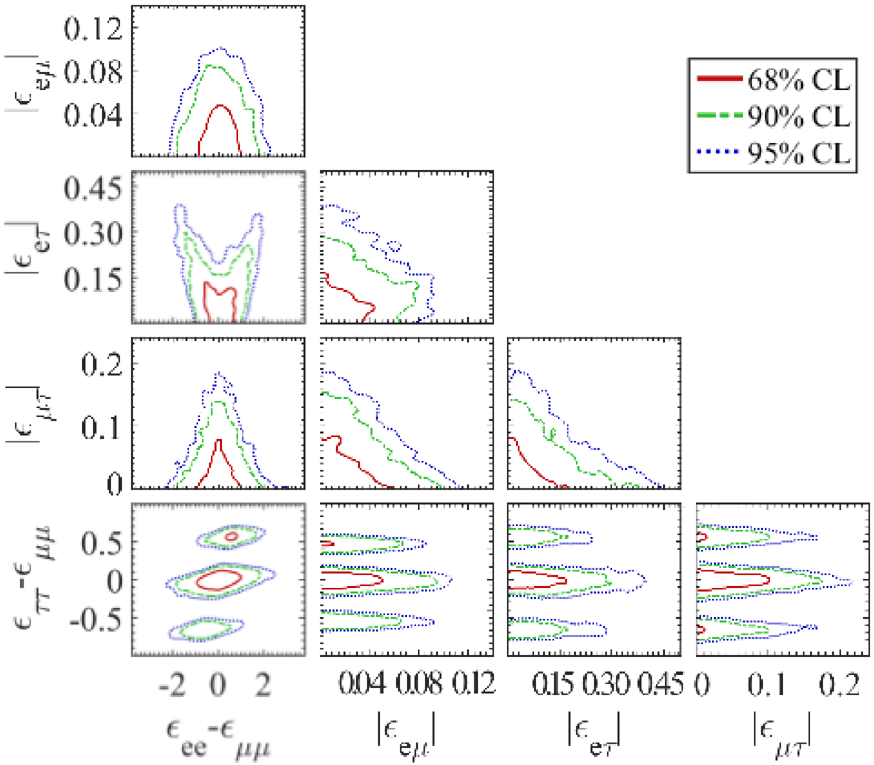

NSI phase sensitivities at DUNE

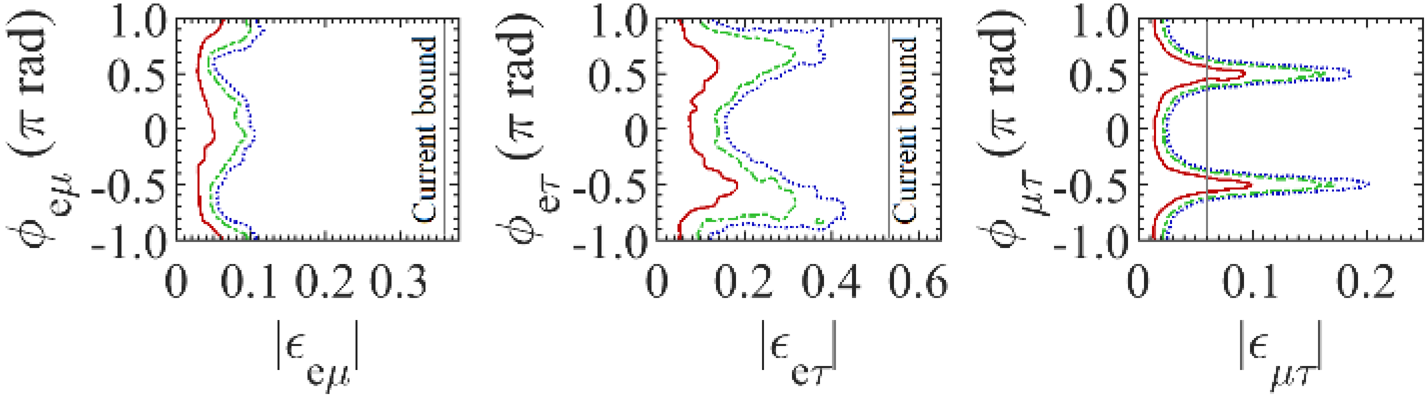

DUNE can improve the current bounds on $\varepsilon_{e\mu}$ and $\varepsilon_{e\tau}$ by over a factor of 2 depending on the value of the phases.

Final remarks

- ❑ NSI can significantly impact on the determination of current unknowns such as CPV and the octant of θ_{23}. Clean determination of the intrinsic CP phase at long-baseline experiments such as DUNE is a formidable task;
- ❑ The sensitivity analysis with tens of parameters currently uses a MCMC and can be improved with AI algorithms;
- ❑ DUNE-BR has a big potential work on the phenomenology studies and the development of simulation+analysis tools for the collaboration.

Thank you!

Appendix

The SM Lagrangian

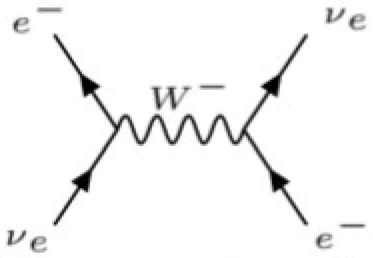

(a) Interação via Corrente Carregada

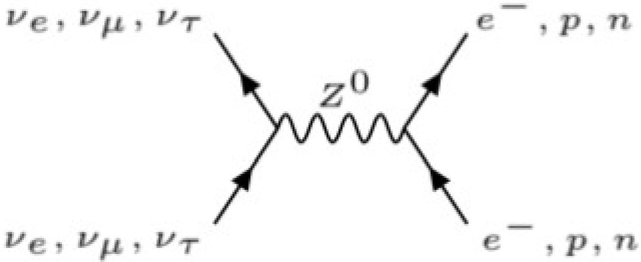

(b) Interação via Corrente Neutra

$$\mathcal{L}_{CC} = -i\left(\frac{-ig}{2\sqrt{2}}\right)[\bar{\nu}_e\gamma^\rho(1-\gamma^5)e]\left(\frac{ig_{\rho\mu}}{m_W^2}\right)\left(\frac{-ig}{2\sqrt{2}}\right)[\bar{e}\gamma^\mu(1-\gamma^5)\nu_e]$$

$$\mathcal{L}_{CN} = \left(\frac{-ig}{2\cos\theta_W}\right)\sum_\alpha[\bar{\nu}_\alpha\gamma^\rho(1-\gamma^5)\nu_\alpha]\left(\frac{i}{m_Z^2}\right)\left(\frac{-ig_{\rho\mu}}{2\cos\theta_W}\right)\sum_f[\bar{f}\gamma^\mu(c_V^f - c_A^f\gamma^5)f]$$

Impact on CP violation sensitivity at DUNE

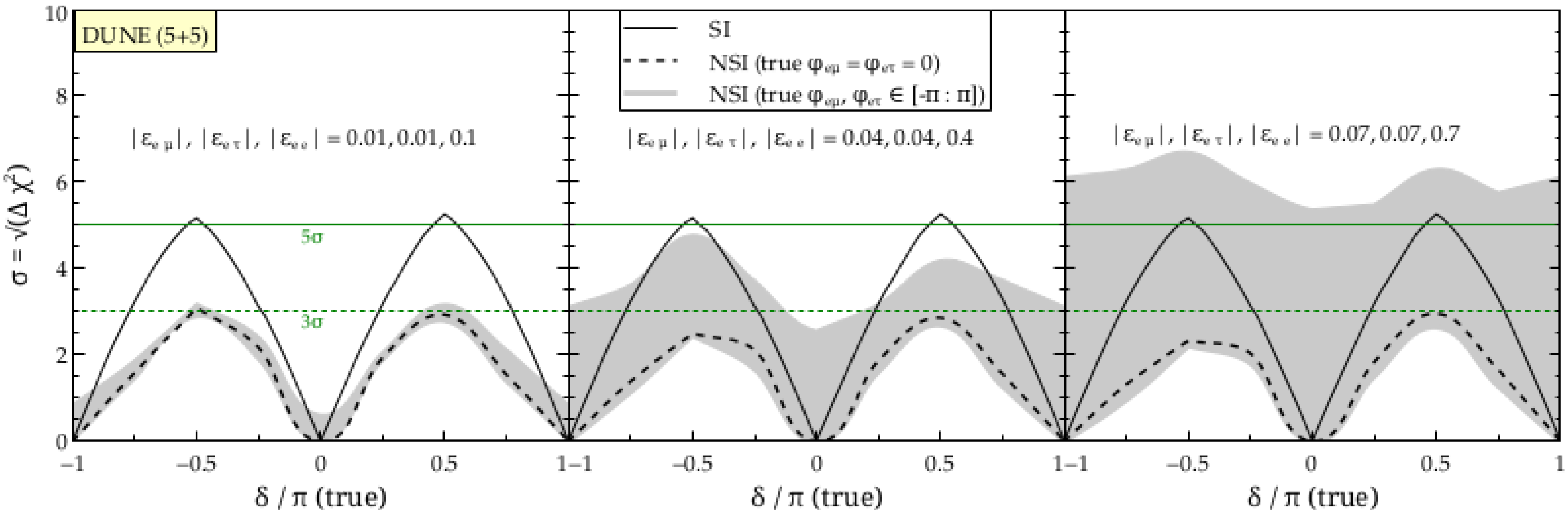

M. Masud and P. Mehta, Phys. Rev. **D94**, 013014 (2016), 1603.01380.

Lorentz Violation

G. Barenboim et al. / Physics Letters B 788 (2019) 308–315

Lorentz violating parameters at DUNE

$$H = H_{Vac} + H_{Mat} + H_{NSI}$$

$$a_{\alpha\beta} = \sqrt{2} G_F N_e \varepsilon_{\alpha\beta}$$

$$H = H_{Vac} + H_{Mat} + H_{LV}$$

$$H_{LV} = \begin{pmatrix} a_{ee} & a_{e\mu} & a_{e\tau} \\ a^*_{e\mu} & a_{\mu\mu} & a_{\mu\tau} \\ a^*_{e\tau} & a^*_{\mu\tau} & a_{\tau\tau} \end{pmatrix} - \frac{4}{3} E \begin{pmatrix} c_{ee} & c_{e\mu} & c_{e\tau} \\ c^*_{e\mu} & c_{\mu\mu} & c_{\mu\tau} \\ c^*_{e\tau} & c^*_{\mu\tau} & c_{\tau\tau} \end{pmatrix}$$

Correlations between the non-diagonal and diagonal CPT-violating parameters at DUNE

G. Barenboim et al. / Physics Letters B 788 (2019) 308–315

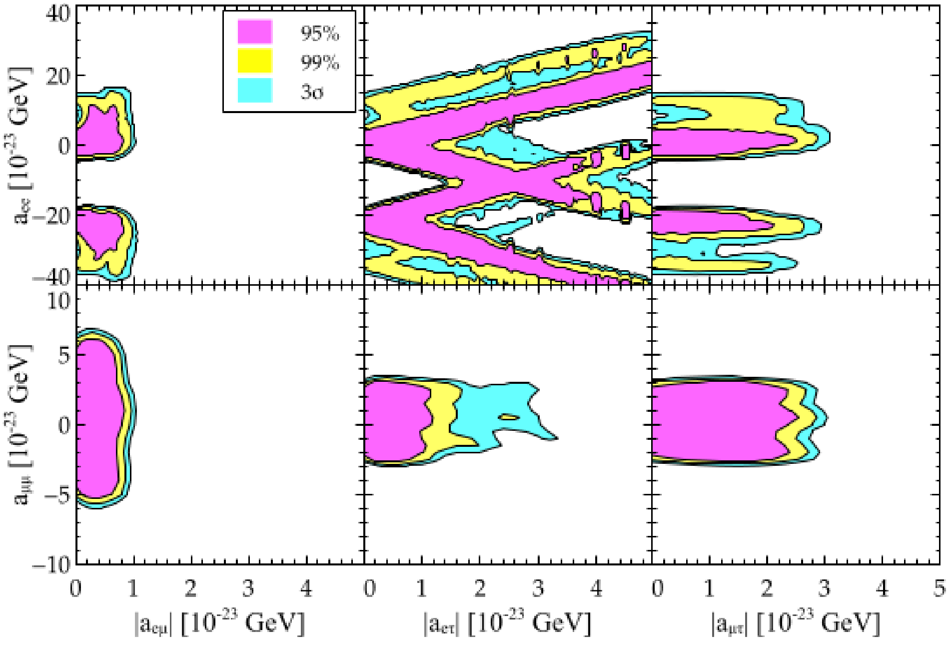

Current bounds:

$\lvert a_{e\mu}\rvert$ [GeV]	2.5×10^{-23}
$\lvert a_{e\tau}\rvert$ [GeV]	5.0×10^{-23}
$\lvert a_{\mu\tau}\rvert$ [GeV]	8.3×10^{-24}

CPT

G. Barenboim et al. / Physics Letters B 780 (2018) 631–637

CPT violation

$$|m^2(K^0) - m^2(\overline{K}^0)| < 0.25 \text{ eV}^2$$

- $P(\nu_\mu \to \nu_e) \neq P(\bar{\nu}_\mu \to \bar{\nu}_e)$ → CP violation
- $P(\nu_\mu \to \nu_\mu) \neq P(\bar{\nu}_\mu \to \bar{\nu}_\mu)$ → CPT violation
- Huge disappearance stats at DUNE.
- Any difference between ν_μ and anti-ν_μ should be clearly visible:

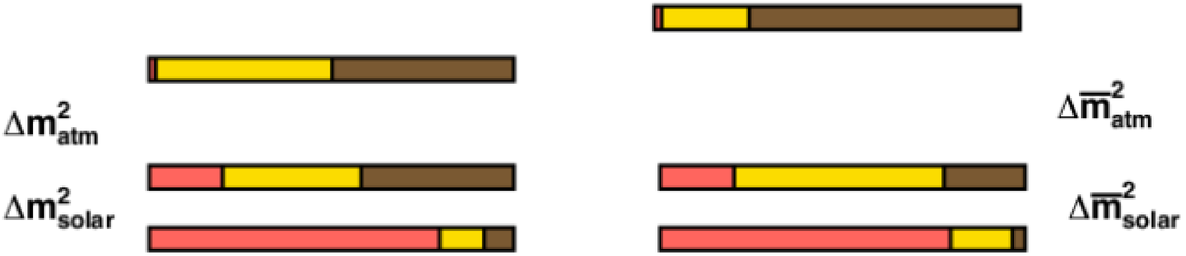

DUNE sensitivity to neutrino-antineutrino parameters difference

$$|\Delta m^2_{21} - \Delta \overline{m}^2_{21}| < 4.7 \times 10^{-5}\,\mathrm{eV}^2,$$
$$|\Delta m^2_{31} - \Delta \overline{m}^2_{31}| < 3.7 \times 10^{-4}\,\mathrm{eV}^2,$$
$$|\sin^2\theta_{12} - \sin^2\overline{\theta}_{12}| < 0.14,$$
$$|\sin^2\theta_{13} - \sin^2\overline{\theta}_{13}| < 0.03,$$
$$|\sin^2\theta_{23} - \sin^2\overline{\theta}_{23}| < 0.32.$$

parameter	value
Δm^2_{21}	$7.56 \times 10^{-5}\mathrm{eV}^2$
Δm^2_{31}	$2.55 \times 10^{-3}\mathrm{eV}^2$
$\sin^2\theta_{12}$	0.321
$\sin^2\theta_{23}$	0.43, 0.50, 0.60
$\sin^2\theta_{13}$	0.02155
δ	1.50π

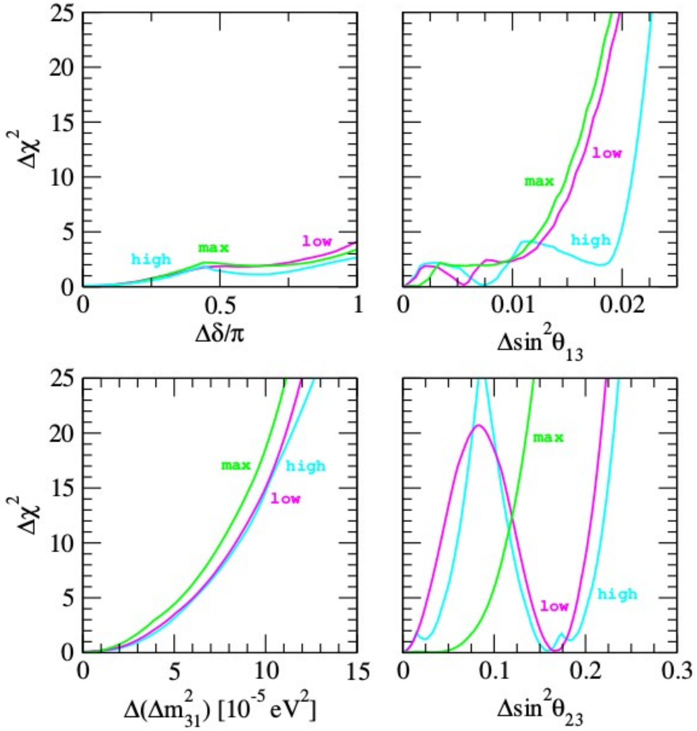

Imposter solutions

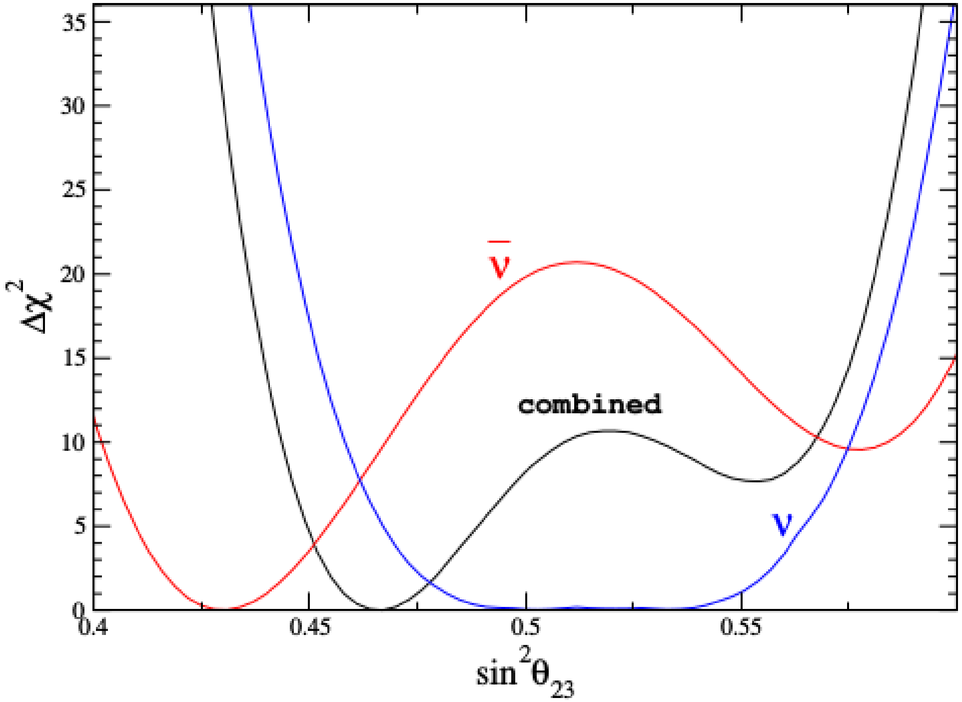

What happens if CPT is not assumed?
For example:
$\sin^2\theta_{23}$ = 0.5
for neutrinos and 0.43 for anti-neutrinos.

The combined analysis gives 0.467 with 3σ and 5σ difference for neutrinos and antineutrinos respectively.

Data set used for CPT violation constraints

- solar neutrino data [Cleveland et al., 1998, Kaether et al., 2010, Abdurashitov et al., 2009, Hosaka et al., 2006, Cravens et al., 2008, Abe et al., 2011, Nakano, 2016, Aharmim et al., 2008, Aharmim et al., 2010, Bellini et al., 2014]: θ_{12}, Δm^2_{21}, θ_{13}
- neutrino mode in long–baseline experiments K2K [Ahn et al., 2006], MINOS [Adamson et al., 2013, Adamson et al., 2014], T2K [Abe et al., 2017a, Abe et al., 2017b] and NOνA [Adamson et al., 2017b, Adamson et al., 2017a]: θ_{23}, Δm^2_{31}, θ_{13}
- KamLAND reactor antineutrino data [Gando et al., 2011]: $\overline{\theta}_{12}$, $\Delta\overline{m}^2_{21}$, $\overline{\theta}_{13}$
- short–baseline reactor antineutrino experiments Daya Bay [An et al., 2017], RENO [Choi et al., 2016] and Double Chooz [Abe et al., 2014]: $\overline{\theta}_{13}$, $\Delta\overline{m}^2_{31}$
- antineutrino mode in long–baseline experiments[1] MINOS [Adamson et al., 2013, Adamson et al., 2014] and T2K [Abe et al., 2017a, Abe et al., 2017b]: $\overline{\theta}_{23}$, $\Delta\overline{m}^2_{31}$ $\overline{\theta}_{13}$

References

[Abdurashitov et al., 2009] Abdurashitov, J. N. et al. (2009). Measurement of the solar neutrino capture rate with gallium metal. III: Results for the 2002–2007 data-taking period. *Phys. Rev.*, C80:015807.

[Abe et al., 2011] Abe, K. et al. (2011). Solar neutrino results in Super-Kamiokande-III. *Phys. Rev.*, D83:052010.

[Abe et al., 2017a] Abe, K. et al. (2017a). Combined Analysis of Neutrino and Antineutrino Oscillations at T2K. *Phys. Rev. Lett.*, 118(15):151801.

[Abe et al., 2017b] Abe, K. et al. (2017b). Updated T2K measurements of muon neutrino and antineutrino disappearance using 1.5×10^{21} protons on target. *Phys. Rev.*, D96(1):011102.

[Abe et al., 2014] Abe, Y. et al. (2014). Improved measurements of the neutrino mixing angle θ_{13} with the Double Chooz detector. *JHEP*, 10:086. [Erratum: JHEP02,074(2015)].

[Adamson et al., 2013] Adamson, P. et al. (2013). Measurement of Neutrino and Antineutrino Oscillations Using Beam and Atmospheric Data in MINOS. *Phys. Rev. Lett.*, 110(25):251801.

[Adamson et al., 2014] Adamson, P. et al. (2014). Combined analysis of ν_μ disappearance and $\nu_\mu \to \nu_e$ appearance in MINOS using accelerator and atmospheric neutrinos. *Phys. Rev. Lett.*, 112:191801.

[Adamson et al., 2017a] Adamson, P. et al. (2017a). Constraints on Oscillation Parameters from ν_e Appearance and ν_μ Disappearance in NOvA. *Phys. Rev. Lett.*, 118(23):231801.

[Adamson et al., 2017b] Adamson, P. et al. (2017b). Measurement of the neutrino mixing angle θ_{23} in NOvA. *Phys. Rev. Lett.*, 118(15):151802.

[Aharmim et al., 2008] Aharmim, B. et al. (2008). An Independent Measurement of the Total Active B-8 Solar Neutrino Flux Using an Array of He-3 Proportional Counters at the Sudbury Neutrino Observatory. *Phys. Rev. Lett.*, 101:111301.

[Aharmim et al., 2010] Aharmim, B. et al. (2010). Low Energy Threshold Analysis of the Phase I and Phase II Data Sets of the Sudbury Neutrino Observatory. *Phys. Rev.*, C81:055504.

[Ahn et al., 2006] Ahn, M. H. et al. (2006). Measurement of Neutrino Oscillation by the K2K Experiment. *Phys. Rev.*, D74:072003.

[An et al., 2017] An, F. P. et al. (2017). Measurement of electron antineutrino oscillation based on 1230 days of operation of the Daya Bay experiment. *Phys. Rev.*, D95(7):072006.

[Bellini et al., 2014] Bellini, G. et al. (2014). Final results of Borexino Phase-I on low energy solar neutrino spectroscopy. *Phys. Rev.*, D89(11):112007.

[Choi et al., 2016] Choi, J. H. et al. (2016). Observation of Energy and Baseline Dependent Reactor Antineutrino Disappearance in the RENO Experiment. *Phys. Rev. Lett.*, 116(21):211801.

[Cleveland et al., 1998] Cleveland, B. T., Daily, T., Davis, Jr., R., Distel, J. R., Lande, K., Lee, C. K., Wildenhain, P. S., and Ullman, J. (1998). Measurement of the solar electron neutrino flux with the Homestake chlorine detector. *Astrophys. J.*, 496:505–526.

[Cravens et al., 2008] Cravens, J. P. et al. (2008). Solar neutrino measurements in Super-Kamiokande-II. *Phys. Rev.*, D78:032002.

[Gando et al., 2011] Gando, A. et al. (2011). Constraints on θ_{13} from A Three-Flavor Oscillation Analysis of Reactor Antineutrinos at KamLAND. *Phys. Rev.*, D83:052002.

[Hosaka et al., 2006] Hosaka, J. et al. (2006). Solar neutrino measurements in super-Kamiokande-I. *Phys. Rev.*, D73:112001.

[Kaether et al., 2010] Kaether, F., Hampel, W., Heusser, G., Kiko, J., and Kirsten, T. (2010). Reanalysis of the GALLEX solar neutrino flux and source experiments. *Phys. Lett.*, B685:47–54.

[Nakano, 2016] Nakano, Y. (2016). PhD Thesis, University of Tokyo. http://www-sk.icrr.u-tokyo.ac.jp/sk/_pdf/articles/2016/doc_thesis_naknao.pdf.